

## Low Voltage Driving of High Xe Pressure PDPs

Shigeo Mikoshiba

Department of Electronic Engineering, The University of Electro-Communications,  
Chofu, Tokyo, Japan, 182-8585  
mikoshiba@ee.uec.ac.jp

**Abstract:** High Xe-content PDPs attain improved luminous efficiency, but with sacrifices of higher sustain and addressing voltages and slower discharge build-up. By examining PDPs with 3.5% - 70% Xe contents, it was revealed that utilization of the space charge priming as well as wall charge accumulation are effective in order to obtain low operating voltages with a high switching speed, especially for higher Xe pressures. The optimum Xe content was found to be 70%, considering efficiency, luminance, and sustain voltage. Also introduced in this paper is a driving technique with 1V data pulse and 30V scan pulse voltages.

**Keywords:** plasma display; efficiency; Xe content.

### Xe Content and Luminous Efficiency

It has been reported that an increase in the Xe content improves the light emission efficiency of PDPs. The Xe content of Ne+Xe mixtures was varied from 3.5% to 100% under the addressed conditions with which an expression of TV images is possible. Luminous efficiency and luminance were measured as functions of sustain pulse voltage ( $V_s$ ) and sustain pulse frequency ( $f$ ).

Figure 1 shows luminous efficiency as functions of  $V_s$  and  $f$  for a Ne+Xe (10%) panel [1,2]. There is a peak in the luminous efficiency with respect to  $V_s$  for each frequency. When  $V_s$  is low, the discharge current build-up is slow and the Xe atoms are not efficiently excited. As  $V_s$  is increased, the efficiency increases. A further increase however causes reduction of efficiency due to an increase in the effective electron temperature. The maximum efficiency is determined by a compromise of stable discharges and avoiding losses by plasma saturation, ion-heating, or non-optimal electron

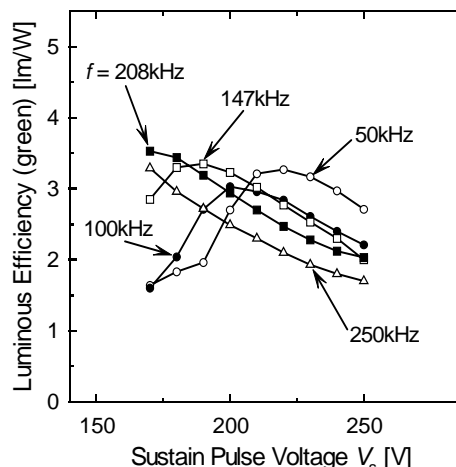


**Figure 1.** Luminous efficiency vs. sustain pulse voltage, Ne+Xe (10%).

temperature. Figure 1 indicates that the maximum luminous efficiencies can be obtained under two kinds of combinations of the drive voltage and frequency; high  $V_s$  and low  $f$  (e.g.,  $V_s=220V$  and  $f=50kHz$ ), or low  $V_s$  and high  $f$  (e.g.,  $V_s=170V$  and  $f=208kHz$ ). For both cases the efficiencies are identical at 3.3 lm/W in green.

Figure 2 shows efficiency vs. sustain pulse voltage for 70% Xe [3]. Just as Fig. 1, there is a peak in the luminous efficiency with respect to  $V_s$  for each frequency. The peak efficiency can be found with high  $V_s$  and low  $f$  ( $V_s=310V$ ,  $f=100kHz$ ), or with low  $V_s$  and high  $f$  ( $V_s=280V$ ,  $f=357kHz$ ). For both cases the values of efficiency maxima are identical, 4.1 lm/W, but higher than those for 10% Xe.

**Table I.** Maximum efficiency for respective Xe contents with optimized  $V_s$  and  $f$ .

Case	Xe content [%]	Optimum sustain pulse voltage [V]	Optimum sustain pulse frequency [kHz]	Pulse width [ $\mu$ s]	Maximum efficiency (green) [lm/W]	Luminance (green) [cd/m <sup>2</sup> ]
1	3.5	150	100	5	2.0	130
2	10	170	250	2	2.5	290
3	20	190	500	1	3.7	1100
4	50	240	500	1	4.7	1900
5	70	290	333	1.5	5.0	3000
6	100	310	333	1.5	5.2	3200

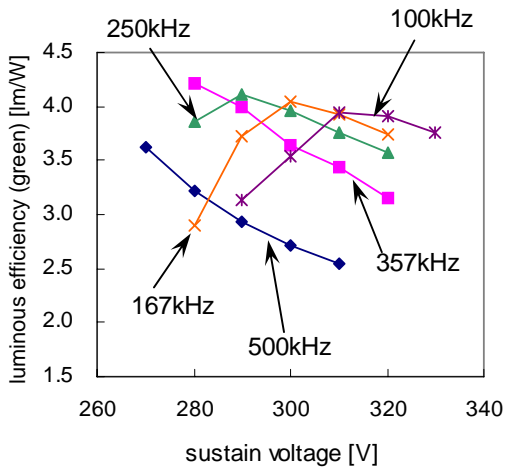


Figure 2. Luminous efficiency vs. sustain pulse voltage, Ne+Xe (70%).

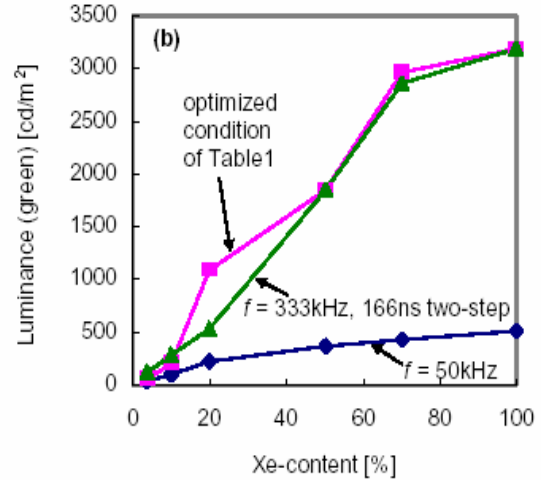


Figure 4. Xe content vs. luminance.

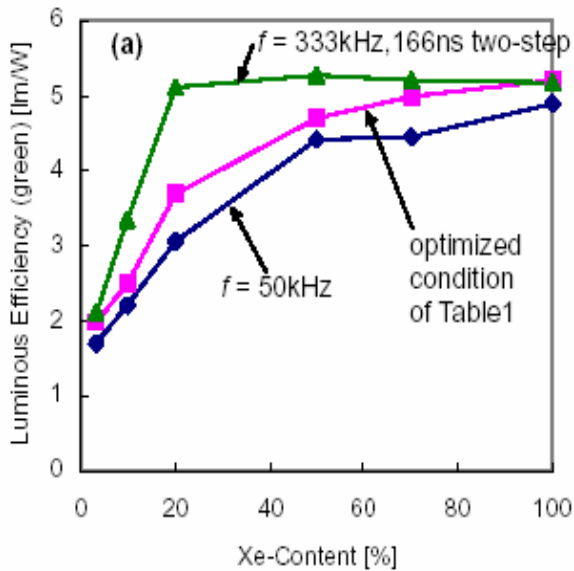


Figure 3. Xe content vs. luminous efficiency.

Table 1 summarizes the maximum luminous efficiency and the associated luminance as well as drive conditions for respective Xe contents [4]. Variations of the maximum efficiency and luminance obtained under the conditions shown in Table I are plotted in Figs. 3 and 4, with the label “optimized condition of Table I.” For reference, efficiencies for  $f=50\text{kHz}$  are also plotted with the label “ $f=50\text{kHz}$ ”. Here,  $V_s$  for each content is optimized. The curves labeled “ $f=333\text{kHz}$ , 166ns two-step” indicates that the panel is driven with two-step pulses of frequency 333kHz and width 166ns [4].

Optimum values of  $V_s$  which yield the maximum efficiency when  $f=250\text{kHz}$  are, 160V, 310V, and 340V

for 10%, 70%, and 100% Xe, respectively. This indicates that  $V_s$  becomes higher as the Xe content is increased.  $V_s$  can be reduced by increasing the sustain pulse frequency, as will be mentioned in the following section. The optimum sustain voltages and frequencies for various Xe contents are plotted in Figs. 5 and 6. The optimum sustain voltage increases as Xe content is increased. The optimum frequency for 70% and 100% Xe contents is 333kHz. The optimum Xe content for a Ne+Xe mixture is found to be 70% considering the efficiency, luminance, and required sustain voltage.

### Sustain Voltage and Sustain Frequency

The sustain pulse voltages which yield the maximum efficiency are shown in Fig. 7 as a function of the sustain pulse frequency. As the Xe content is increased, a field-to-pressure ratio decreases, ionization efficiency lowers, and hence higher voltage is necessary. The voltage that yields the efficiency peak increases as the frequency is reduced and Xe content is increased.

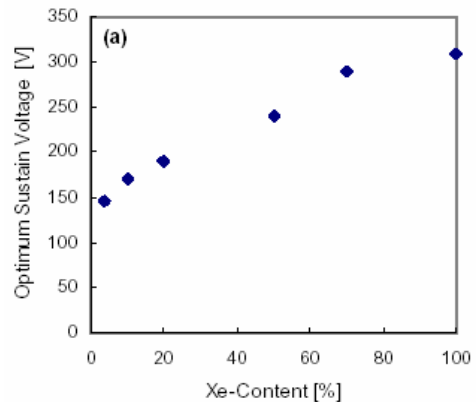


Figure 5. Xe content vs. optimum sustain voltage.

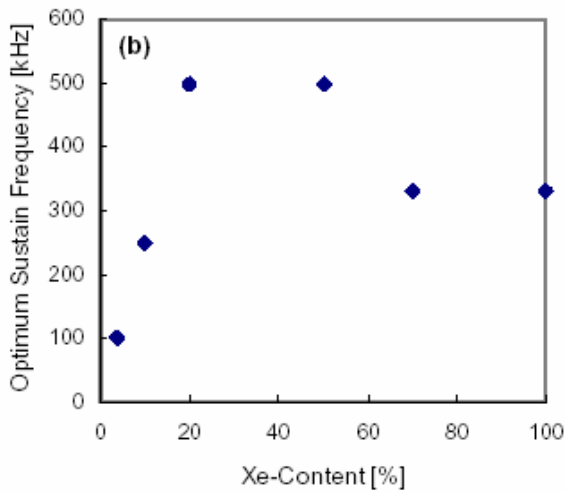


Figure 6. Xe content vs. optimum sustain frequency.

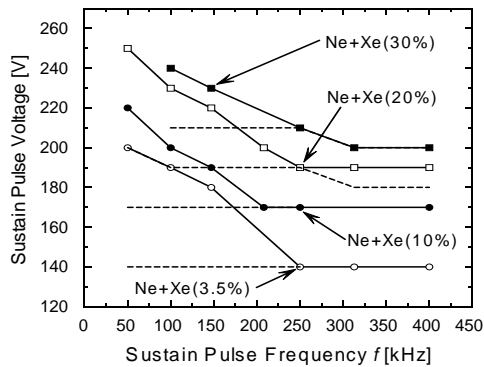


Figure 7. Minimum sustain pulse voltages (broken lines) and optimum sustain pulse voltages for obtaining maximum efficiency (solid lines).

The minimum sustain pulse voltages are also indicated by the broken lines. These voltages become independent of the drive frequency as the frequency becomes high enough. An increase in the sustain pulse voltage associated with an increase in the Xe content can be suppressed by increasing the sustain pulse frequency. The pulse repetition becomes faster and a portion of the space charges created by the previous pulse remains until the following pulse is applied. Due to the priming effect of these space charges, the discharge current build-up becomes faster so that Xe atoms are excited more efficiently with lower voltage.

### Space Charge Effect on Addressing

Figure 8 shows the minimum address voltage,  $|V_{scan}| + V_{data}$ , as a function of the scan pulse width,  $\tau_{scan}$ , for 3.5% and 30% Xe contents. The figure is obtained when there were neither wall charges nor priming particles. Therefore the case represents the write addressing scheme. As the Xe content is increased from 3.5% to 30%, the address voltage increases from 230V to 345V, by 115V. Also the minimum  $\tau_{scan}$  to initiate

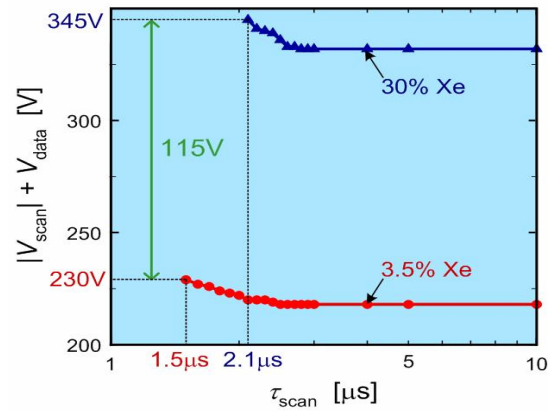


Figure 8. Address voltage,  $|V_{scan}| + V_{data}$ , for write addressing without priming charges.

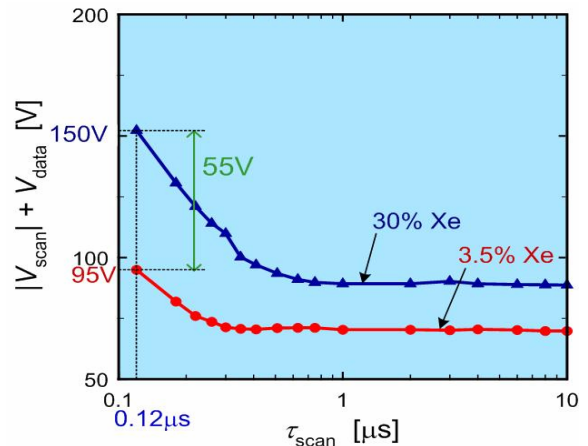
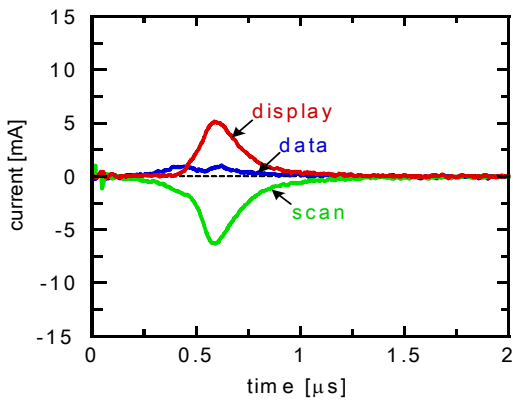


Figure 9. Address voltage,  $|V_{scan}| + V_{data}$ , for erase addressing with priming charges.

the breakdown becomes longer, from 1.5 $\mu$ s to 2.1 $\mu$ s. Figure 9 shows the address voltages when abundant priming charges are provided, representing the erase addressing scheme. As the Xe content is increased from 3.5% to 30%, the address voltage increases from 85V to 150V, but by only 55V. The minimum  $\tau_{scan}$  is 0.12 $\mu$ s, independent of the Xe content. These indicate that a use of an erase addressing scheme, rather than the write addressing scheme, is preferable when driving high Xe content PDPs.

When the scan discharge is ignited in a Xe 3.5% panel with the scan voltage -60V under a condition that there are abundant priming particles, the discharge current waveforms through the display, scan, and data electrodes become those shown in Fig. 10. There is only small current flowing through the data electrodes. However for a Xe 50% panel with the scan and data voltage



**Figure 10.** Discharge current waveforms through display, scan, and data electrodes. 3.5% Xe panel,  $V_{scan} = -60V$ ,  $V_{display} = V_{data} = 0$ .

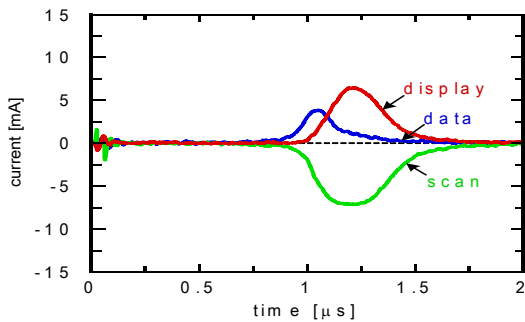


**Figure 11.** Discharge current waveforms through display, scan, and data electrodes. 50% Xe panel,  $V_{scan} = -68V$ ,  $V_{display} = V_{data} = 0$ .

-68V, a discharge is first established between the scan and data electrodes, and then it is transferred between the scan and display electrodes, Fig. 11. Considering that the distances between the scan and address electrodes is  $120\mu m$ , which is longer than the distance between the sustain and scan electrodes of  $70\mu m$ , the figures indicate that the priming effect is more pronounced for high Xe content panels.

### Accumulation of Wall Charges

The address voltage can also be reduced by providing wall charges prior to an application of the scan and data pulses. The vertical axis of Fig. 12 ( $V_{test1}$ ) shows the voltage required for the addressing and the horizontal axis is the voltage of wall charge accumulation pulse ( $V_{priming0}$ ) which is applied prior to the addressing [5]. As the priming pulse width  $\tau_{priming}$  becomes wider,  $V_{test1}$  becomes lower. This implies that more wall charges are accumulated with wider priming pulse since a sufficient time is provided for the discharge build-up as well as

diffusion/drift of the space charges to the cell walls. The curves of Fig. 12 can be divided into 3 regions. The vertical dotted lines apply to the case when  $\tau_{priming}=40\mu s$ . Region (1) is when  $V_{priming0}$  is relatively low and self-erase discharges do not take place at the trailing edge of the pulse. The wall voltage in this region becomes equal to  $V_{priming0}$  and hence we obtain,

$$V_{priming0} + V_{test1} = V_{breakdown} \text{ (constant).}$$

The decrement of  $V_{test1}$  and increment of  $V_{priming0}$  are identical. In region (2), the decrement of  $V_{test1}$  becomes smaller than the increment of  $V_{priming0}$ . This implies that a portion of the wall charges is eliminated due possibly to a weak, non-self-sustained discharge, or due to surface recombination of the wall charges. These dissipations of the wall charges assess the lower limit of the addressing voltages. In region (3),  $V_{test1}$  increases abruptly, indicating that a self-sustained, self-erase discharge is

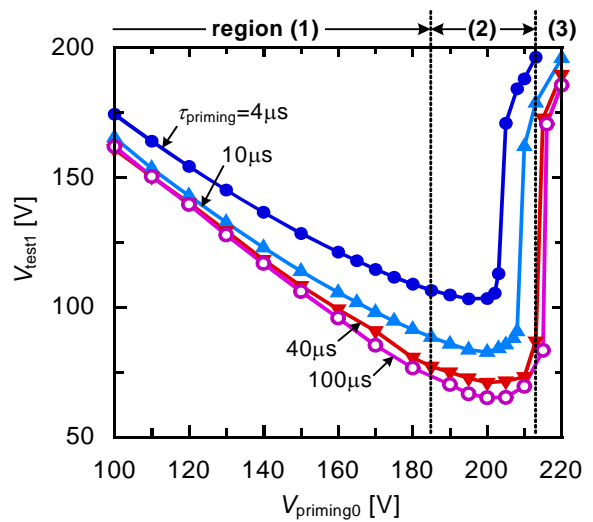


**Figure 12.** Minimum value of  $V_{test1}$  that causes the discharge breakdown as a function of priming pulse voltage which accumulates the wall charges.

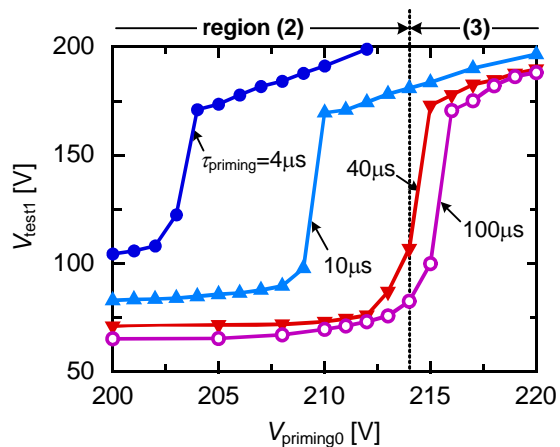


**Figure 13.** Magnified view of Fig. 12 around the border of regions (2) and (3).

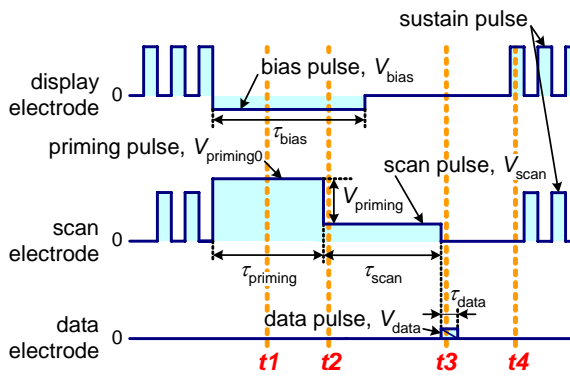


**Figure 14.** Erase-addressing pulse voltage waveforms utilizing the self-erase discharge threshold.

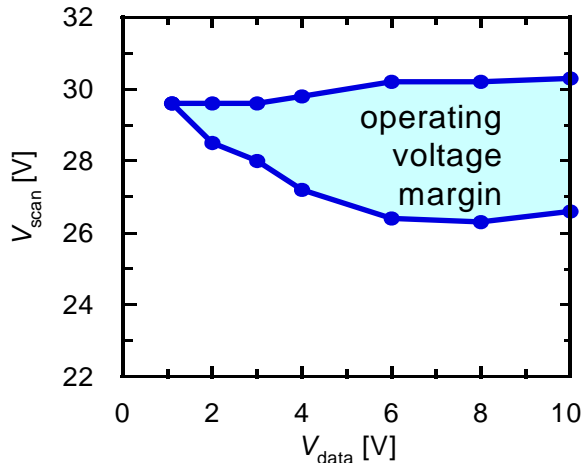


**Figure 15.** Operating voltage margin for  $V_{scan}$  and  $V_{data}$ .

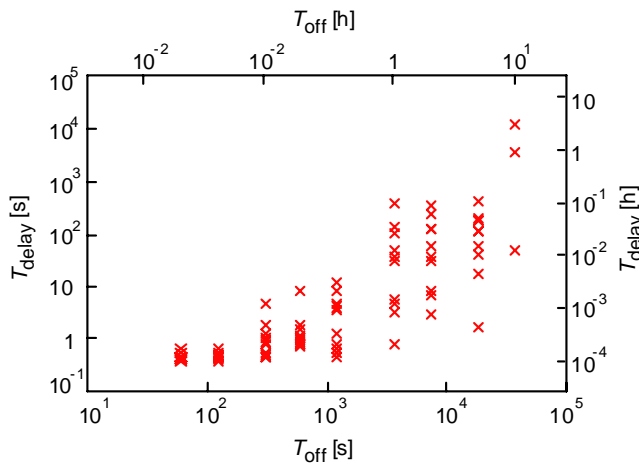


**Figure 16.** Discharge delay time,  $T_{delay}$ , as a function of discharge OFF period,  $T_{off}$ , for 3.5% Xe panel.

established and almost all the wall charges are eliminated. The border of the regions (2) and (3) is enlarged in Fig. 13. Near the dotted line for  $\tau_{priming}=40\mu s$ ,  $V_{test1}$  increases from 107V to 173V when  $V_{priming0}$  increases from 214V to 215V. This implies that the self-erase discharge can be triggered by an infinitesimal increase of priming and data voltages.

### Low Voltage Addressing with Self-Erase-Discharge Threshold

By utilizing the sharp voltage threshold of the self-erase discharge, the data and scan voltages can be reduced appreciably. The voltage waveforms for the drive scheme are shown in Fig. 14. Here,  $V_{priming} + V_{scan} = V_{priming0}$ . Prior to the addressing, the priming pulse discharge with  $V_{priming0} = 214V$  is generated ( $t_1$  of Fig. 14). Then the wall charges corresponding to 214V are accumulated. This value is slightly lower than the threshold of the self-erase discharge, namely the border voltage of regions (2) and (3). At the end of the priming pulse,  $t_2$ , the voltage is dropped not to 0 but to  $V_{scan}$ , by the amount  $V_{priming} = 184V$ . This voltage is the value at the boarder of regions (1) and (2). The magnitude of the scan pulse is as large as the width of region (2). At time  $t_2$ , there is no discharge. Therefore the wall charges accumulated by the priming pulse are preserved. When the scan voltage drops from  $V_{scan}$  to 0 at  $t_3$ , a weak discharge is ignited between the data and scan electrodes.

An application of a data pulse in synchronous with the weak discharge at  $t_3$  triggers an intense, self-erase discharge between the display and scan electrodes. Since the discharge eliminates all the wall charges, no sustain discharges take place at  $t_4$ . On the other hand when the data pulse is not applied, there is no self-erase discharge and the sustain discharges are ignited at  $t_4$ . This is the erase addressing scheme. Unlike the ordinary write- or erase-addressing scheme, however, the scan and data pulses are not applied simultaneously. Instead, the weak discharge after the trailing edge of the scan pulse coincides with the data pulse. Figure 15 shows the operating voltage margins for  $V_{scan}$  and  $V_{data}$ . The data and scan pulse voltages can be reduced to 1 and 30 volts, respectively, by utilizing the sharp threshold of self-erase-discharge ignition, provided that the panel has perfectly uniform voltage characteristics.

### Role of Exoelectrons for Discharge Ignition

In order to realize a high dark-room-contrast-ratio, the set-up discharges should be reduced only once in a TV field of 16.7ms. This means that priming electrons, even a small quantity, should be provided during the TV field time. Space charges and metastable atoms diffuse to the cell walls and lost within less than 0.1ms. The horizontal axis of Fig. 16,  $T_{off}$ , denotes the time between the two voltage pulses. The first pulse generates a discharge to excite MgO. The second pulse is to measure the priming effect by the exoelectrons. The degree of the priming is measured by the delay,  $T_{delay}$ , of the discharge initiation of the second pulse. With less priming electrons, the discharge requires longer time to be ignited [6]. The measured values of  $T_{delay}$  keeps increasing even after 10 hours, implying that there still are electron emission after

the initial excitation of MgO. Thus, a use of MgO is important because of its exoelectron emission capability,

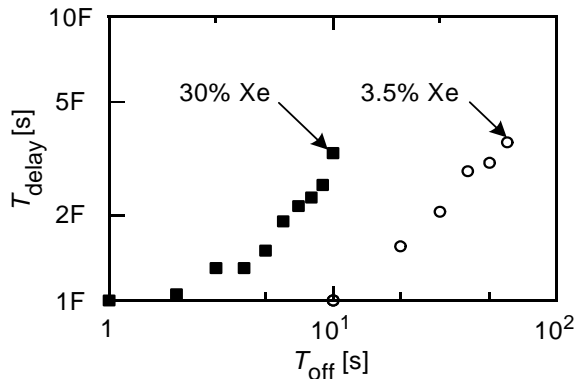


Figure 17.  $T_{delay}$  vs.  $T_{off}$  for 3.5% and 30% Xe.

in addition to high secondary electron emission.

$T_{delay}$  is shown again in Fig. 17 with  $T_{off}$  ranging from 1s to 100s. The vertical axis is plotted in a unit of the TV field time, F, which is 16.7ms. For 3.5% Xe, the discharge initiates from the first field if  $T_{off}$  is less than 10s, namely if a completely dark TV image does not continue for more than 10s. For 30% Xe,  $T_{off}$  should be less than 1s for the discharge to start from the first TV field. This indicates that there is less amount of exoelectron emission for high Xe panels.

### Conclusions

It was experimentally found that the optimum Xe content for the high luminance, efficiency, and low sustain voltage is 70% in Xe-Ne mixture. The sustain voltage can be reduced while keeping the efficiency high by increasing

the sustain frequency. With an introduction of the priming particles, the statistical time lag of the discharge triggering for the 30% is reduced and becomes approximately equal to that of 3.5%. Once triggered, the formative time lag of the discharge and also diffusion/drift of the space charges is shorter, and hence accumulation speed of the wall charges is faster for higher Xe contents. A sharp threshold of the self-erase discharge ignition can be adopted for low voltage addressing of  $V_{data}=1V$  and  $V_{scan}=30V$ , provided that all the discharge cells in a panel is perfectly uniform.

### References

1. G. Oversluizen, *et al.*, "High-Xe-content high-efficacy PDPs," *J. SID*, vol. 12, no. 1, pp. 51-55, 2004.
2. T. Minami, *et al.*, "High-frequency drive of high-Xe-content PDPs for high-efficiency and low-voltage performance," *J. SID*, vol. 12, no. 2, pp. 191-197, 2004.
3. S. Mikoshiba, "Features of High Xe Content PDPs," *Proc. IDMC '05*, pp. 75-78, 2005.
4. H. Kanazawa, *et al.*, "Light Emission Characteristics of PDPs for Xe Concentrations Ranging from 3.5% to 100%," *EuroDisplay '05*, pp. 272-275, 2005.
5. A. Saito, *et al.*, "Feasibility of Driving PDPs with 1-Volt Data and 30-Volt Scan Pulses by Utilizing Self-Erase-Discharge Threshold," *IDW/AD'05*, pp. 1449-1452, 2005.
6. T. Shiga, *et al.*, "Exoelectron Emission from MgO and Ultra-High Contrast Drive of PDPs," *SID '05 Digest*, pp. 1248-1251, 2005.